Desalination and Water Treatment
www.deswater.com

doi: 10.1080/19443994.2015.1006826

57 (2016) 268–277
January

Taylor & Francis
Taylor & Francis Group

Photocatalytic degradation of *tert*-butyl alcohol and *tert*-butyl formate using palladium-doped zinc oxide nanoparticles with UV irradiation

Zaki S. Seddigi[a], Saleh A. Ahmed[b,*], Ali Bumajdad[c], Mohammed A. Gonadal[d], Ekram Y. Danish[e], Ahmed M. Shawky[f], Naeema H. Yarkandi[b]

[a]*Faculty of Public Health and Health Informatics, Department of Environmental Health, Umm Al-Qura University, Makkah 21955, Saudi Arabia, Tel. +966 504947677; email: zsseddigi@uqu.edu.sa*
[b]*Faculty of Applied Sciences, Chemistry Department, Umm Al-Qura University, Makkah 21955, Saudi Arabia, Tel. +966 530435760; email: saleh_63@hotmail.com (S.A. Ahmed)*
[c]*Faculty of Science, Chemistry Department, Kuwait University, P.O. Box 5969 Safat 13060, Kuwait, Kuwait, Tel. +965 99411998; email: a.bumajdad@ku.edu.kw*
[d]*Laser Research Group, Physics Department & Center of Excellence in Nanotechnology, King Fahd University of Petroleum and Minerals, Dhahran 31261, Saudi Arabia, Tel. +966 556211252; email: magondal@kfupm.edu.sa*
[e]*Faculty of Science, Chemistry Department, King Abdulaziz University, Jeddah, Saudi Arabia, Tel. +966 505610204; email: eydanish@kau.edu.sa*
[f]*Science and Technology Unit (STU), Umm Al-Qura University, Makkah 21955, Saudi Arabia, Tel. +966 566382285; email: shawkius@hotmail.com*

Received 5 October 2014; Accepted 16 November 2014

ABSTRACT

Methyl *tert*-butyl ether (MTBE) is a well-known environmental pollutant. Its removal from water bodies is a challenge associated with ensuring the chemical is present only within the prescribed limits. *Tert*-butyl alcohol (TBA) and *tert*-butyl formate (TBF) are the two main intermediate (stable and toxic) compounds that are obtained during the decomposition of MTBE. The accumulation of these intermediates in water bodies raises serious issues about their chemical toxicity, as they are suspected carcinogens in humans. In this work, palladium-doped zinc oxide is utilised as a photocatalyst to decompose these contaminants in the presence of UV light. These photocatalysts have been found to efficiently degrade 100 ppm aqueous solutions of TBA and TBF using 100 mg of each of these photocatalysts and UV irradiation over a period of five hours.

Keywords: Methyl *tert*-butyl ether; *Tert*-butyl alcohol; *Tert*-butyl formate, Photocatalyst; Photocatalyst; Photodegradation; Zinc oxide

*Corresponding author.

Presented at the International Conference on Business, Economics, Energy and Environmental Sciences (ICBEEES) 19–21 September 2014, Kuala Lumpur, Malaysia

1. Introduction

Methyl *tert*-butyl ether (MTBE) has been used in the United States since the 1970s as an octane enhancer, replacing lead in mid- and high-quality gasoline. The reformulated gasoline contains approximately 11–15% MTBE by volume (approximately 2.7% by weight) [1–4]. Subsequently, this reformulated gasoline has been used worldwide, and due to is large scale usage and for other reasons, such as accidental spills, leakage in storage tanks and pipelines, etc., groundwater has become contaminated with MTBE [5–8]. MTBE is a polar compound that is not easily absorbed into soils, is highly soluble in water and possesses a lower density than water. As a result, MTBE easily contaminates groundwater. Moreover, the presence of MTBE also increases the solubility of many aromatic compounds (contained in gasoline) in water through the co-solvent effect, another potentially harmful effect [9]. The widespread presence of MTBE in surface water, groundwater and treated water has attracted great interest from the scientific community and health agencies due to its potential human carcinogenicity [10]. Though the use of MTBE has been banned in the United States, it is still highly utilised in other parts of the world. Even in the event that MTBE were to be banned worldwide, there is still the challenge associated with addressing the degradation of the MTBE already released into the environment. There are many reports on how to degrade MTBE using biological, chemical and advanced oxidation methods. As a result, the scientific community has taken notice that some of the degradation intermediates of MTBE are toxic, potentially carcinogenic and more stable than MTBE itself [11–14]. *Tert*-butyl alcohol (TBA) is also a fuel oxygenate and is commonly found as a co-contaminant along with MTBE in groundwater. TBA is a co-product of MTBE manufacturing and an important degradation by-product of MTBE [15–17]. It is highly soluble in water and therefore moves throughout the groundwater system. Presently, TBA has been listed as a United States EPA priority pollutant. However, in states such as California and New Jersey, its presence in drinking water has been restricted to 12 and 100 μg/L, respectively [18–20]. TBA is also a known toxin and a suspected human carcinogen. Its presence in water has raised serious concerns in the scientific community about its treatment and degradation [21,22]. TBA has unique physical properties including high water solubility, a low adsorption tendency and a lower Henry's constant than MTBE, which hinders treatment by conventional means. Treatment methods such as adsorption over activated carbon and air stripping have been found to be ineffective for TBA removal from contaminated water. It is important to note that TBA has a lesser tendency than MTBE to be attracted to activated carbon surfaces. Due to TBA's low Henry's constant, it cannot be effectively and easily removed using the air stripping method, in which a very high air/water ratio is required to reach the desired efficiency. The biodegradation of TBA has also been reported to be less effective than MTBE, which biodegrades to TBA in water. Therefore, TBA is likely to accumulate in groundwater. Failure of the aforementioned conventional treatment methods to effectively remove TBA has forced the scientific community to search for alternative methods to solve this serious problem. *Tert*-butyl formate (TBF) is also a major intermediate produced during biodegradation, chemical oxidation and advanced oxidation of MTBE [23,24]. TBF has been detected in exhaust emissions from automobiles using MTBE containing reformulated gasoline [25].

Recently, advanced oxidation processes (AOPs) have garnered intense interest for their removal of toxic compounds from contaminated water. AOPs involve combinations of ozone (O_3), hydrogen peroxide (H_2O_2), ultraviolet light (UV), and metal oxide semiconductors (e.g., TiO_2, ZnO, etc.) [26,27]. The main advantage of AOPs is attributed to the formation of a hydroxyl radical (**.**OH), which non-specifically attacks almost any organic compound with a very high reaction rate constant. In addition, the **.**OH oxidises a large number of organic toxic pollutants into nontoxic intermediates and end products (CO_2 and H_2O), compared to conventional treatment methods, such as activated carbon and air stripping, where pollutants are transferred from water to another medium that may need further treatment before final disposal [28]. There are only a few reports that have focused primarily on the treatment and removal of TBA contaminated water using AOPs [20,22]. Dindar and Icli [29] used Fenton's reagent method to degrade TBA and other MTBE degradation intermediates. Eslami et al. used a ZnO/UV/H_2O_2 process to degrade TBA during the degradation of MTBE until complete mineralisation was achieved [30].

In this work, we consider the various environmental concerns posed by TBA and TBF. From our recent reports [2–4,10] on the photocatalytic degradation of MTBE in water using Pd-doped zinc oxide, where identified TBA and TBF as the main intermediates produced from the photocatalytic degradation of MTBE. Therefore, the main objective of this study is to photocatalytically degrade TBA and TBF in an aqueous solution in the presence of UV light and a Pd-doped zinc oxide in a batch reactor.

2. Material and methods

MTBE, TBA, and TBF from Sigma-Aldrich, double distilled water, palladium nitrate and zinc oxide (ZnO) (J.T. Baker, USA) photocatalyst were used during this work.

2.1. Preparation of the catalyst

The palladium (Pd) doping of ZnO was performed by the well-established incipient wetness impregnation method [31–35]. In a typical procedure, the required amount of precursor salt for Pd (palladium nitrate) was dissolved in de-ionised water to prepare a solution of an incipient volume. Later, the required volume of palladium nitrate solution was added to solid ZnO powder. The mixture was kept undisturbed at room temperature for an hour and dried at 100°C overnight. The sample was then calcined at 450°C for 3 h before being cooled to room temperature to obtain the final catalyst.

2.2. Characterisation techniques

The synthesised photocatalyst samples were characterised using advanced instrumentation techniques. Scanning electron microscopy (SEM) and transmission electron microscopy (TEM) of the samples were performed to determine the morphology and size of the particles. The X-ray diffraction patterns were obtained using an X-ray diffractometer equipped with a monochromatic high-intensity Cu K radiation (=1.5418 Å, 40 kV, 100 mA). The X-ray photoelectron spectroscopy (XPS) surface elemental analysis was conducted using a Thermo ESCALAB 250 Xi with Al K Alpha radiation (1486.6 eV). Spectrum acquisition and processing were performed using Thermo Advantage Software, version 4.58. The binding energy was referenced to the C1 s line at 284.6 eV for calibration. The sample was introduced into the preparation chamber with the sample holder and degassed until a good vacuum was achieved. Then, the sample was transferred to the analysis chamber where the vacuum was set to 9–10 mBar. The analyses were performed using the

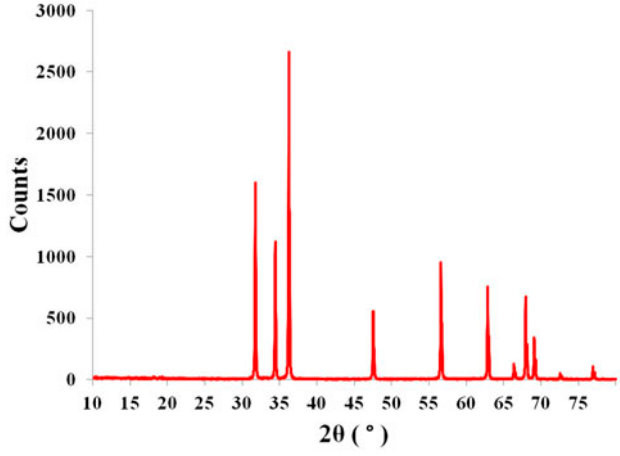

Fig. 1. XRD diffractogram of the 1.0% doped ZnO photocatalyst.

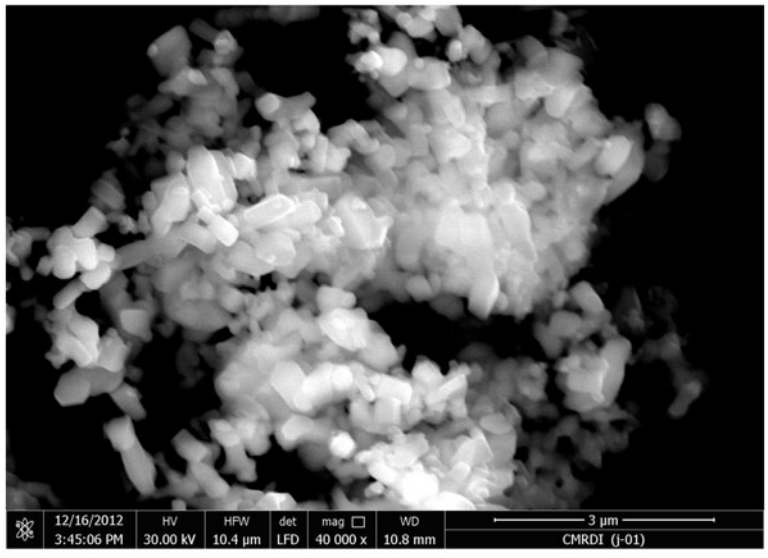

Fig. 2. SEM micrograph of the 1.0% Pd-doped ZnO photocatalyst.

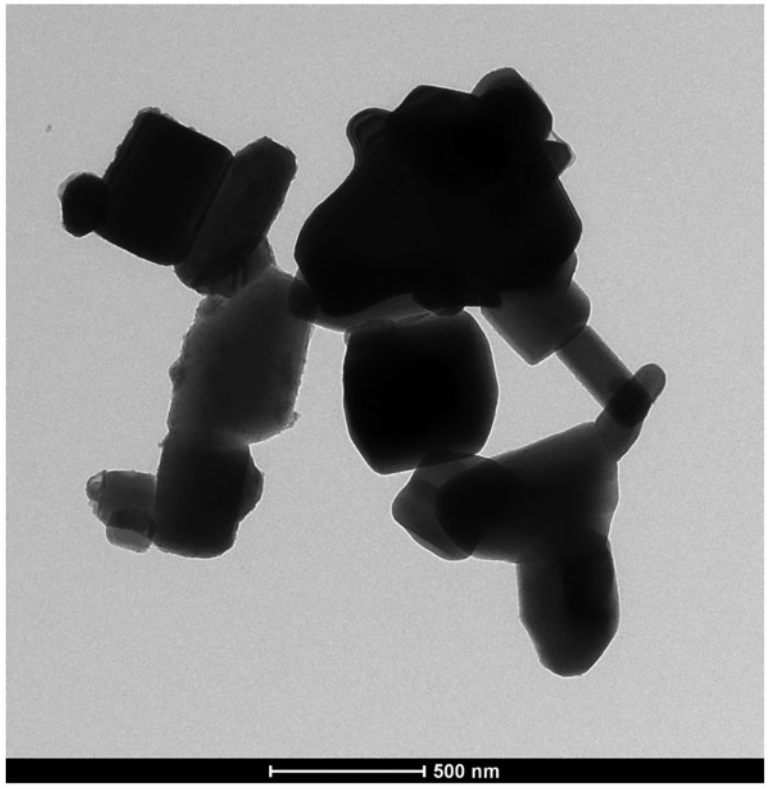

Fig. 3. TEM micrograph of the 1.0% Pd-doped ZnO photocatalyst.

Table 1
BET Surface areas, pore volumes and pore sizes for the different prepared Pd/ZnO

Sample	SBET m/g	Pore volume cm/g	Pore size nm
0.5% Pd/ZnO	4.34	0.009	8.8
1.0% Pd/ZnO	4.08	0.009	8.9
1.5% Pd/ZnO	3.16	0.011	13.4

following parameters: a pass energy of 20 eV, a dwell time 50 ms and a step size 0.1 eV. A standard charge compensation mode flood gun was employed to neutralise the charge build up on the surface of the insulating samples.

The nitrogen (N_2) adsorption-desorption isotherms were determined at the liquid nitrogen temperature (−195˚C) using an automatic ASAP 2010 Micromeritics sorptiometer equipped with an outgassing platform and an on-line data acquisition and handling system operating standard BET [36] and BJH [37] analytical software for the adsorption data following the experimental recommendations that were previously reported [36]. The 99.999% pure N_2 gas was purchased from KOAC (Kuwait), and the test samples (Cerias - 300 ± 2 mg) were pre-outgassed at 110˚C and 5–10 Torr for 3 h. The reproducibility of the adsorption–desorption isotherms was determined to be better than 95%.

2.3. Photocatalytic reaction procedure

A batch photoreactor made of quartz and equipped with cooling jacket was used for the photocatalytic degradation reaction of TBA and TBF. A high pressure mercury UV lamp was placed in the photoreactor. A volume of 350 mL of 100 ppm of MTBE, TBA and TBF in distilled water was transferred into the photoreactor and 100 mg of each of the photocatalysts, including 0.5% Pd-doped ZnO, 1.0% Pd-doped ZnO and 1.5% Pd-doped ZnO were added to each reaction

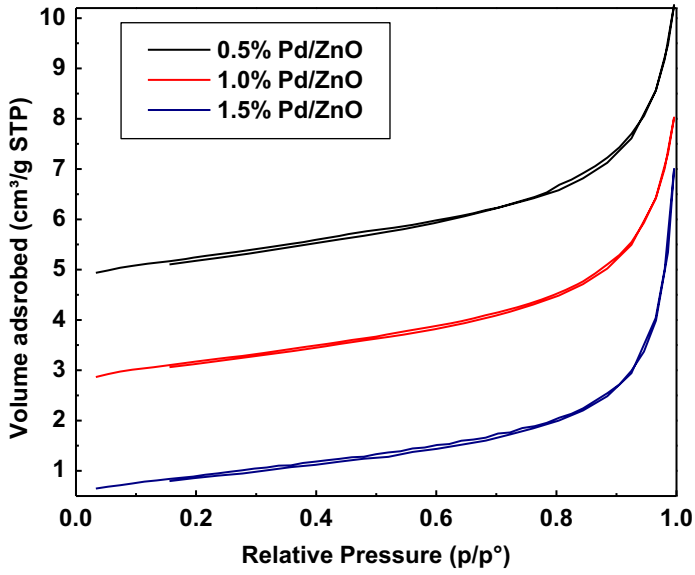

Fig. 4. N_2 adorption-desorption isotherms for the different synthesised Pd/ZnO samples.

mixture. The temperature of the reaction mixtures was controlled by a cold water stream at a temperature of 18 ± 1°C during the irradiation process. The reaction mixtures were stirred for half an hour to achieve homogeneity with oxygen gas (O_2) passed through the reactor at a moderate flow rate over a period of half an hour. Then, the O_2 flow was stopped and the UV lamp was turned on and allowed to glow for a few minutes in open air before placing it inside the photoreactor. The experimental setup was covered with an aluminium foil and left for a period of five hours. A sample was collected at the end of every hour during that period.

3. Results and discussion

3.1. X-ray diffraction studies

X-ray diffractogram of the 1% Pd-doped zinc oxide is shown in Fig. 1. Specified 2θ peaks from the diffractogram are observed at 31.77705 (100), 34.43169 (002), 36.2632 (101), 47.55247 (102), 56.60973 (110), 62.86751 (103), 67.95329 (112), and 69.09436 (201). These are rounded to two digits significant figures, permitting confirmation of the hexagonal wurtzite structure of ZnO from the diffractogram [38–40]. It also important to mention that Pd peaks could not be determined from the XRD diffractogram and at the same time, no specific changes were observed in the diffraction pattern of the ZnO nanoparticles. This can be attributed to the small amount of particles, their small size and their homogeneous distribution [2].

3.2. Electron microscopy studies of the photocatalysts

The size and the shape of the particles of the photocatalyst play an important role in its activity. Therefore, FESEM and TEM were both used to study the shape and the size of ZnO particles doped with 1% Pd. The morphology of these nanoparticles is shown in Fig. 2 and is cubic/cuboid in shape despite being

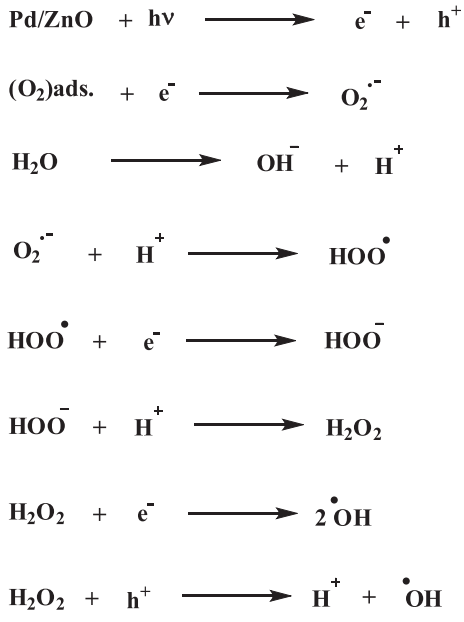

Fig. 5. Proposed mechanism for the formation of hydroxyl radicals using a photoexcitation reaction.

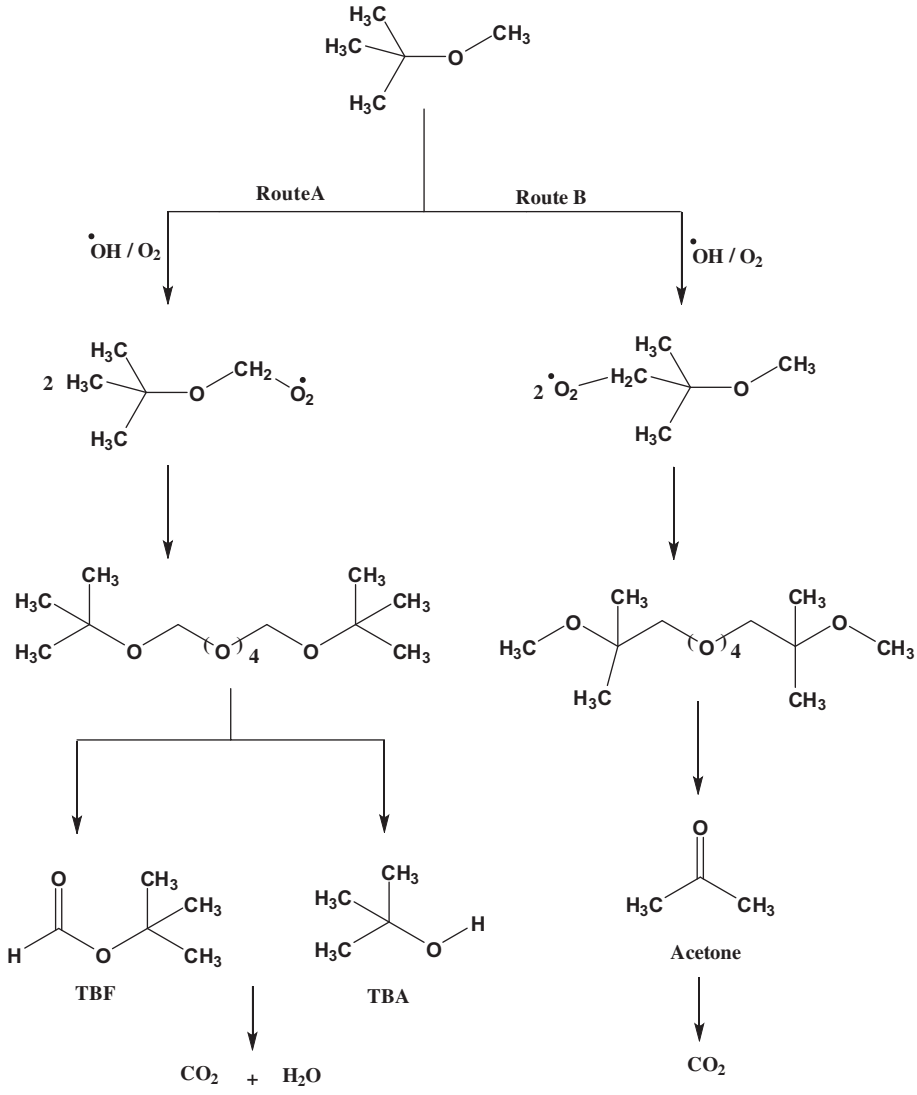

Fig. 6. Proposed mechanism for the formation of TBA, TBF and acetone from the photodegradation of MTBE and the path to the final products.

different sizes. Due to their small numbers, the Pd nanoparticles could not be observed by SEM on the surfaces of the ZnO nanoparticles. To overcome this limitation, TEM was employed. The TEM micrograph of the 1% Pd-doped ZnO photocatalysts are shown in Fig. 3.

3.3. N_2 adorption-desorption isotherms

As shown in Table 1, upon doping the ZnO with Pd, the surface area tended to decrease slightly as the concentration of Pd increased, which suggests that the Pd dopant enhances the growth of the particle size. All three samples exhibit a type III isotherm, which shows a low N_2 uptake at a low relative pressure (as seen in Fig. 4). This indicates that the studied samples exhibit weak interactions between the adsorbate (N_2) and the adsorbent (Pd/ZnO). The absence of clear hysteresis in the three samples indicates a very low porosity (as shown in the reported pore volume in Table 1). The surface characterisation of the different amounts of Pd revealed that the optimal amount of Pd is 1% and any greater amount causes the surface area and the intensity of the XPS peaks to decrease.

3.4. Photocatalytic degradation study

Recently, we presented work on the photocatalytic degradation of MTBE when exposed to UV light in the presence of Pd-doped ZnO as a photocatalyst [10].

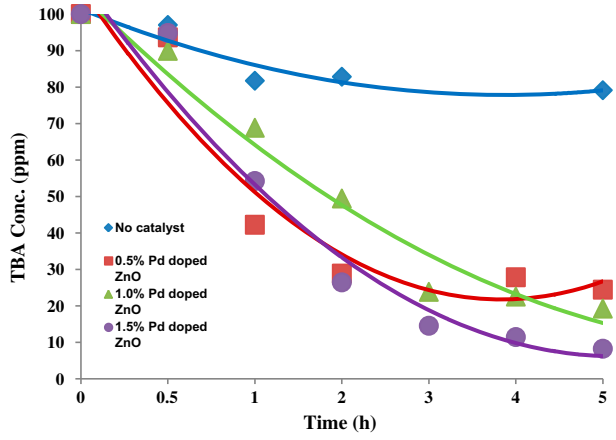

Fig. 7. Photocatalytic degradation of TBA in the presence of a series of photocatalysts.

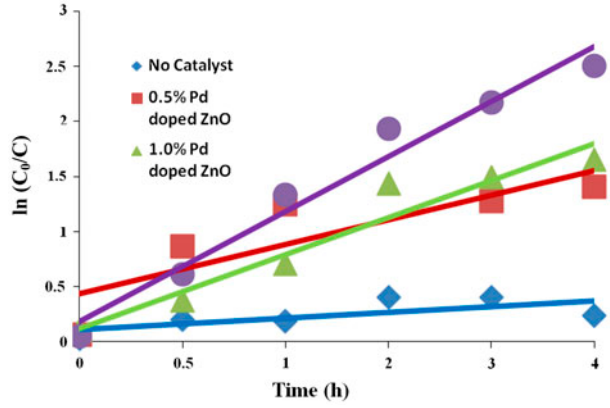

Fig. 9. Kinetics of the photocatalytic degradation of TBA in the presence of a series of photocatalysts.

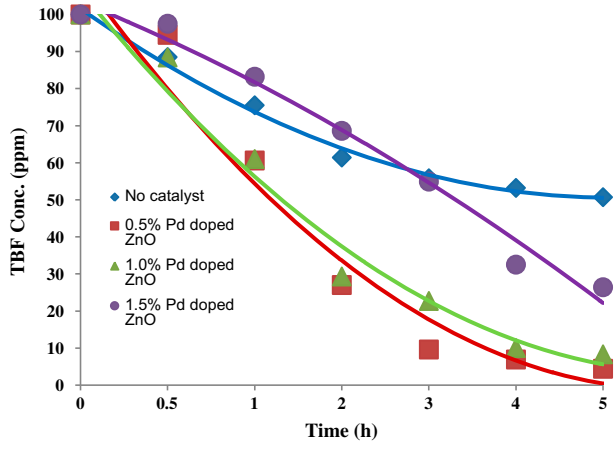

Fig. 8. Photocatalytic degradation of TBF in the presence of a series of photocatalysts.

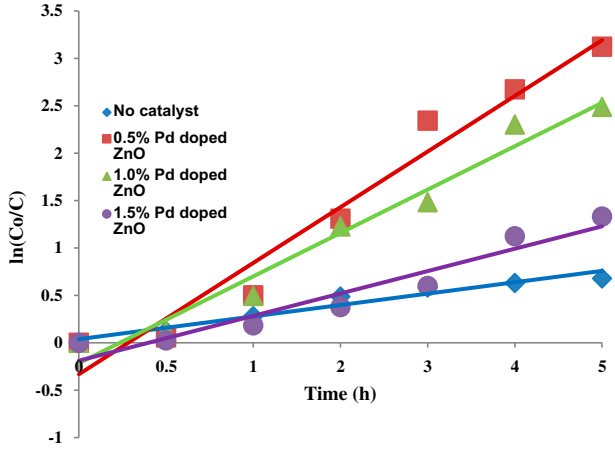

Fig. 10. Kinetics of the photocatalytic degradation of TBF in the presence of a series of photocatalysts.

Here, we mainly report on the photocatalytic degradation of TBA, TBF and acetone, which have been identified as the main intermediates resulting from MTBE degradation. The GC-MS chromatogram of the MTBE degradation in the presence of UV light and the Pd-doped ZnO is shown in Fig. 6 and the mass spectra of the intermediates are shown in Figs. 1–3 of the supplementary material.

The photocatalytic degradation of TBA and TBF in water was studied utilising a series of (0.5, 1.0, and 1.5%) Pd-doped ZnO as photocatalysts. Photocatalytic degradation data were obtained from these catalysts when they were irradiated with UV light for a period of five hours. The ZnO doped with 1.5% Pd was found to have the most effective photoactivity against the TBA and the 0.5% Pd-doped ZnO was found to be most efficient against the TBF. This is may be attributed to the selectivity of the catalysts toward the photodegradation of both the two pollutants.

In the presence of this catalyst, almost complete degradation of the TBA and the TBF was achieved. Therefore, Pd-doped ZnO can be considered an effective photocatalyst for the degradation of TBA and TBF to carbon dioxide and water

Initially, the rate of the photodegradation of the TBA and the TBF was found to be very fast, as seen in Figs. 7 and 8, respectively. This can be attributed to the sufficient availability of the hydroxyl radicals created by UV irradiation (Fig. 5).

However, as the reaction proceeds with time, different intermediates are formed and compete with the TBA and TBF parent molecules at consuming the

hydroxyl radicals. As a result, the rate of the photocatalytic degradation reaction decreases. Another proposed mechanism for the formation of the TBA, TBF and acetone and then their decomposition into carbon dioxide and water is presented in Fig. 6. The increased efficiency of the Pd-doped ZnO is due to the fast transfer of the photoexcited electrons from the surface of the semiconducting photocatalyst to the Pd metal surface, which acts as an electron reservoir [41–43]. Consequently, the recombination process of the photogenerated electrons and holes is efficiently controlled due to the presence of the Pd metal on the catalyst surface [44]. This halt in the recombination of photoexcited species increases the photocatalytic activity of the catalyst [45,46].

3.5. The kinetic studies of the photodegradation of TBA and TBF

The process of heterogeneous photocatalysis starts with the adsorption of the organic contaminant molecules on the surface of the photocatalyst [40–42]. These adsorbed molecules react with the hydroxyl radicals (**.**OH) that form as a result of the reaction between the water and the photogenerated species (electrons/holes). The heterogeneous photocatalytic degradation of the organic pollutants in water behaves according to the kinetic model proposed by Langmuir-Hinshelwood [33]. Accordingly, the rate of the photocatalytic degradation of the organic pollutant is proportional to the surface area covered on the photocatalyst by the organic pollutant molecules:

$$\text{Rate(R)} = -(\mathrm{d}C/\mathrm{d}T)\alpha\theta \quad (1)$$

$$k_r\theta = (k_rKC/1 + KC) \quad (2)$$

If $KC << 1$, KC becomes negligible, and:

$$-\ln(C/C_0) = K_{app}t \quad (3)$$

where θ, K, k_r and C are the surface coverage, the adsorption coefficient of the reactant, the reaction rate constant and the concentration of the reactant, respectively. If the concentration C becomes very low (corresponding to a significantly diluted solution), KC is much less than 1. A plot of $\ln(C_0/C)$ vs. the irradiation time (T) yields a straight line, corresponding to a first order reaction. The rate constant for the reaction can be obtained from the slope of the plot (see Figs. 9 and 10). The rate constant of the photodegradation reaction is highest for the 1.5% Pd-doped ZnO and the 0.5% Pd-doped ZnO for TBA and TBF, respectively.

4. Conclusion

In this work, the photocatalytic degradation of TBA and TBF in water was studied using both ZnO and Pd-doped ZnO as photocatalysts. Almost complete removal of the TBA and TBF was achieved within five hours using 1.5% Pd-doped ZnO and 0.5% Pd-doped ZnO, respectively. The efficient removal of TBA and TBF is due to the higher concentration of hydroxyl radicals and to the presence of Pd, which controls the recombination of the photogenerated electron/hole (e^-/h^+) pairs.

Acknowledgements

The authors wish to acknowledge the support of King Abdul Aziz City for Science and Technology (KACST) through the Science and Technology Unit at the Umm Al-Qura University for funding project No. 10-wat1240-10 as part of the National Science, Technology and Innovation Plan. Many thanks due to Dr Shahid P. Ansari for helping with some data collection.

References

[1] M.N. Siddiqui, M.A. Gondal, Nanocatalyst support of laser-induced photocatalytic degradation of MTBE, J. Environ. Sci. Health., Part A 49 (2014) 52–58.
[2] Z.S. Seddigi, A. Bumajdad, S.P. Ansari, S.A. Ahmed, E.Y. Danish, N.H. Yarkandi, S. Ahmed, Preparation and characterization of Pd doped ceria–ZnO nanocomposite catalyst for methyl tert-butyl ether (MTBE) photodegradation, J. Hazard. Mater. 264 (2014) 71–78.
[3] Z.S. Seddigi, S.A. Ahmed, S.P. Ansari, N.H. Yarkandi, E. Danish, A. Abu Alkibash, S. Ahmed, The effect of loading of zninc oxide with palladium on the photocatalytic degradation of methyl tert-butyl ether (MTBE) in water, Photochem. Photobiol. 90 (2014) 491–495.
[4] Z.S. Seddigi, S.A. Ahmed, S.P. Ansari, N. Yarkandi, E. Danish, M. Oteef, M. Cohelan, S. Ahmed, A. Abu Alkibash, Photocatalytic degradation of methyl *tert*-butyl ether (MTBE): A review, Adv. Environ. Res. 3 (2014) 11–28.
[5] C. Baus, H. Hung, F. Sacher, M. Fleig, H.-J. Brauch, MTBE in drinking water production occurrence and efficiency of treatment technologies, Acta Hydroch. Hydrob. 33 (2005) 118–132.
[6] J. Arana, A. Pena Alonso, J.M. Dona Rodrıguez, J.A. Herrera Melian, O. Gonzalez Dıaz, J. Perez Pena, Comparative study of MTBE photocatalytic degradation with TiO_2 and Cu-TiO_2, Appl. Catal. B 78 (2008), 355–363.
[7] Y.-J. An, D.H. Kampbell, M.L. Cook, Co-occurrence of MTBE and benzene, toluene, ethylbenzene, and xylene compounds at marinas in large reservoir, J. Environ. Eng. 128 (2002) 902–906.
[8] T. Miyake, T. Shibamoto, Formation of formaldehyde from methyl tert-butylether (MTBE) upon UV irradiation, Bull. Environ. Contam. Toxicol. 62 (1999) 416–419.

[9] C.S. Chen, P.S.C. Rao, J.J. Delfino, Oxygenated fuel induced cosolvent effects on the dissolution of polynuclear aromatic hydrocarbons from contaminated soil, Chemosphere 60 (2005) 1572–1582.
[10] Z.S. Seddigi, S.A. Ahmed, S.P. Ansari, E. Danish, A. Abu Alkibash, S. Ahmed, Kinetics and photodegradation study of aqueous methyl tert-butyl ether using zinc oxide: The effect of particle size, Inter. J. Photoenergy 2013 (2013) 7 pp.
[11] M.S. Callén, M.T. Cruz, S. Marinov, R. Murillo, M. Stefanova, A.M. Mastral, Flue gas cleaning in power stations by using electron beam technology. Influence on PAH emissions. Fuel Process. Technol. 88 (2007) 251–258.
[12] J.M. Miller, D.G. Allen, Modelling transport and degradation of hydrophobic pollutants in biofilters biofilms, Chem. Eng. J. 113 (2005) 197–204.
[13] A. Fischer, M. Müller, J. Klasmeier, Determination of Henry's law constant formethyl tert-butyl ether (MTBE) at groundwater temperatures, Chemosphere 54 (2003) 689–694.
[14] G. Mascolo, R. Ciannarella, L. Balest, A. Lopez, Effectiveness of UV- pollutionin the groundwater: A laboratory investigation, J. Hazard. Mater. 152 (2008) 1138–1145.
[15] J.M. Suflita, M.R. Mormile, Anaerobic biodegradation of known and potential gasoline oxygenates in the terrestrial subsurface, Environ. Sci. Technol. 27 (1993) 976–978.
[16] J.P. Salanitro, L.A. Diaz, M.P. Williams, H.L. Wisniewski, Isolation of a bacterial culture that degrades methyl *t*-butyl ether, Appl. Environ. Microbiol. 60 (1994) 2593–2596.
[17] R.J. Steffan, K. McClay, S. Vainberg, C.W. Condee, D.L. Zhang, Biodegradation of the gasoline oxygenates methyl tert-butyl ether, ethyl tert-butyl ether, and tert-amyl methyl ether by propane-oxidizing bacteria, Appl. Environ. Microbiol. 63 (1997) 4216–4222.
[18] California Department of Health Services. Available from <http://www.dhs.ca.gov/ps/ddwem/AL/actionlevels.htm> (updated March 2003).
[19] New Jersey Department of Environmental Protection. Available from <http://www.state.nj.us/dep/wmm/sgwqt/is_text.html> (updated May 2003).
[20] K. Li, D.R. Hokanson, J.C. Crittenden, R.R. Trussell, D. Minakata, Evaluating UV/H_2O_2 processes for methyl *t*ert-butyl ether and *t*ert-butyl alcohol removal: Effect of pretreatment options and light sources, Water Res. 42 (2008) 5045–5053.
[21] J.D. Cirvello, A. Radovsky, J.E. Heath, D.R. Farnell, C. Lindamood, Toxicity and carcinogenicity of tert-butyl alcohol in rats and mice following chronic exposure in drinking water, Toxicol. Ind. Health 11 (1995) 151–166.
[22] T. Garoma, M.D. Gurol, Degradation of tert-butyl alcohol in dilute aqueous solution by an O_3/UV process, Environ. Sci. Technol. 38 (2004) 5246–5252.
[23] G.T. Hickman, J.T. Novak, Relationship between subsurface biodegradation rates and microbial density, Environ. Sci. Technol. 23 (1989) 525–532.
[24] P.M. Bradley, J.E. Landmeyer, F.H. Chapelle, Aerobic mineralization of MTBE and tert-butyl alcohol by stream-bed sediment microorganisms, Environ. Sci. Technol. 33 (1999) 1877–1879.
[25] H.-O. Shin, T.-S. Kim, Analysis of tert-butanol, methyl tert-butyl ether, benzene, toluene, ethylbenzene and xylene in ground water by headspace gas chromatography–mass spectrometry, Bull. Korean Chem. Soc. 30 (2009) 3049–3052.
[26] S.S. Shinde, P.S. Shinde, C.H. Bhosale, K.Y. Rajpure, Zinc oxide mediated heterogeneous photocatalytic degradation of organic species under solar radiation, J. Photochem. Photobiol. B 104 (2011) 425–433.
[27] M.S.M. Chan, R.J. Lynch, Photocatalytic degradation of aqueous methyl tert-butyl ether (MTBE) in a supported catalyst reactor, Environ. Chem. Lett. 1 (2003) 157–160.
[28] Q. Hu, C. Zhang, Z. Wang, Y. Chen, K. Mao, X. Zhang, Y. Xiong, M. Zhu, Photodegradation of methyl tert-butyl ether (MTBE) by UV/H_2O_2 and UV/TiO_2, J. Hazard. Mater. 154 (2008) 795–803.
[29] B. Dindar, S. Icli, Unusual photoreactivity of zinc oxide irradiated by concentrated sunlight, J. Photochem. Photobiol. 140 (2001) 263–268.
[30] S. Devipriya, S. Yesodharan, Photocatalytic degradation of pesticide contaminants in water, Sol. Energy Mater. Sol. Cells 86 (2005) 309–348.
[31] A.A. Burbano, D.D. Dionysiou, T.L. Richardson, M.T. Suidan, Degradation of MTBE intermediates using fenton's reagent, J. Environ. Eng. 128 (2002) 799–805.
[32] A. Eslami, S. Nasseri, B. Yadollahi, Photocatalytic degradation of methyl tert-butyl ether (MTBE) in contaminated water by ZnO nanoparticles, J. Chem. Technol. Biotechnol. 83 (2008) 1447–1453.
[33] T. Garoma, M.D. Gurol, L. Thotakura, O. Osibodu, Degradation of *t*ert-butyl formate and its intermediates by an ozone/UV process, Chemosphere 73 (2008) 1708–1715.
[34] S. Brunauer, P.H. Emmett, E. Teller, Adsorption of gases in multimolecular layers, J. Am. Chem. Soc. 60 (1938) 309–319.
[35] Elliott P. Barrett, Leslie G. Joyner, Paul P. Halenda, The determination of pore volume and area distributions in porous substances. I. computations from nitrogen isotherms, J. Am. Chem. Soc. 73 (1951) 373–380.
[36] A. Bumajdad, M.I. Zaki, J. Eastoe, L. Pasupulety, Characterization of nano-cerias synthesized in microemulsions by N_2 sorptiometry and electron microscopy, J. Colloid Interface Sci. 302 (2006) 501–508.
[37] K. Hayat, M.A. Gondal, M.M. Khaled, S. Ahmed, A.M. Shemsi, Nano ZnO synthesis by modified sol gel method and its application in heterogeneous photocatalytic removal of phenol from water, Appl. Catal., A 393 (2011) 122–129.
[38] J. Liqiang, Q. Yichun, W. Baiqi, L. Shudan, J. Baojiang, Y. Libin, F. Wei, F. Honggang, S. Jiazhong, Review of photoluminescence performance of nano-sized semiconductor materials and its relationships with photocatalytic activity, Sol. Energy Mater. Sol. Cells 90 (2006) 1773–1787.
[39] C.-C. Chan, C.-C. Chang, W.-C. Hsu, S.-L. Wang, J. Lin, Photocatalytic activities of Pd-loaded mesoporous TiO_2 thin films, Chem. Eng. J. 152 (2009) 492–497.
[40] M. Jakob, H. Levanon, Charge distribution between UV-irradiated TiO_2 and gold nanoparticles. Determination of shift in the fermi level, Nano Lett. 3 (2003) 353–358.

[41] B. Neppolian, A. Bruno, C.L. Bianchi, M. Ashokkumar, Graphene oxide based Pt-TiO_2 photocatalyst: Ultrasound assisted synthesis. Characterization and catalytic efficiency, Ultrason. Sonochem. 19 (2012) 9–15.
[42] W. Xiaohong, D. Xianbo, Q. Wei, H. Weidong, J. Zhaohua, Enhanced photo-catalytic activity of TiO_2 films with doped La prepared by micro-plasma oxidation method, J. Hazard. Mater. B. 137 (2006) 192–197.
[43] N. Tabassum, U. Rafique, K.S. Balkhair, M.A. Ashraf, Chemodynamics of methyl parathion and ethyl parathion: Adsorption models for sustainable agriculture, Biomed. Res. Int. 2014 (2014) 1–8.
[44] M.I. Aguilar, J. Sáez, M. Lloréns, A. Soler, J.F. Ortuño, V. Meseguer and A.Fuentes, Improvement of coagulationflocculation process using anionic polyacryalmide as coagulant aid, Chemosphere 58 (2005) 47–56.
[45] S.I. Abou-Elela, M.E. Ali, H.S. Ibrahim, Combined treatment of retting flax wastewater using fenton oxidation and granular activated carbon, Arab. J. Chem. (In press).
[46] M.L. Davis, D.A. Cornwell, Introduction to Environmental Engineering, third ed., McGraw-Hall, New York, NY, 1998.